

# NUMERICAL ANALYSIS OF FREE VIBRATION OF CROSS-PLY THICK LAMINATED COMPOSITE CYLINDRICAL SHELLS BY CONTINUOUS ELEMENT METHOD

Ta Thi Hien, Tran Ich Thinh, Nguyen Manh Cuong  
*Hanoi University of Science and Technology, Vietnam*

**Abstract.** This paper presents the vibration analysis of thick laminated composite cylindrical shells by a new approach using the Continuous Element Method (CEM). Based on the analytical solutions for the differential equations of thick composite cylindrical shell taking into account shear deflection effects, the dynamic transfer matrix is built from which natural frequencies are easily calculated. A computer program is developed for performing numerical calculations and results from specific cases are presented. Numerical results of this work are compared with published analytical and Finite Element Method (FEM) results. Through different examples, advantages of CEM are confirmed: reduced size of model, higher precision, reduced time of computation and larger range of studied frequencies.

**Keywords:** Free vibration, continuous element method, dynamic stiffness matrix, thick laminated composite cylindrical shell, dynamic transfer matrix.

## 1. INTRODUCTION

With the increasing use of composites as structural elements, studies on the vibration of laminated composite cylindrical shells receive a considerable attention. In the literature, various solution methods based on different beams, plates and shells theories have been applied to the vibration analysis of metallic and composite structures: analytical approaches [1, 2, 3, 4], mode superposition method [5], spline function method [6], wave-train closure principle [7], Rayleigh–Ritz method [8], finite element method (FEM) [9, 10] etc.

The FEM is certainly one of the most popular methods used for analyzing composite structures. However, it is well known that a sufficiently large number of finite elements is inevitable in order to obtain reliable structural dynamic responses owing to their high flexibility and large size, especially at high frequency. Thus it may require high cost as well as a great amount of computer time. Furthermore, the modal analysis used in conjunction with the FEM is limited to frequency regimes where the relative spacing of natural frequencies remains large compared with the relative parameter uncertainty [11]. Thus, recently, special techniques such as equivalent continuum method [12, 13], dynamic stiffness method [5, 14], transfer matrix method [15, 16], spectral element method [17] and

continuous element method (CEM) [18, 19, 20] have been proposed to cope with such difficulties. In direct line, the CEM can be related to the dynamic stiffness method using the characteristic functions of structures. Elementary or refined theories which take into account many effects (inertia, shear, warping, etc.) for beams as well as for plates and shells can be used. In the framework of an elastodynamic theory and with a given set of boundary conditions, it is possible, for a simple, element geometry (for example, rectangular or triangular plate), to obtain the exact solution of the vibration problem [21]. More recently, several kinds of continuous element have been presented for dynamic analysis of some metallic structures. These elements concern straight isotropic beams, curved beams [21], isotropic thin plates [18] and isotropic axisymmetric shells [19]. In [19] a procedure to obtain the dynamic stiffness matrix of an axisymmetric shell is presented. The dynamic stiffness relationship is written according to a series expansion of the displacement and force components and an integration of the dynamic transfer relationship. In the above-mentioned works, the lack of discretization implied that loadings had to be defined on boundaries. The topology of the structure and the layout of the concentrated loads location determined the necessary number of continuous elements to be used. The procedure presented in [19] was extended to the case of distributed loads in the recent paper [20].

To the authors' knowledge, in the literature available, no numerical solutions have been presented for the study on free vibration of thick laminated composite cylindrical shells by using CEM.

This paper presents a continuous element model based on the first-order shear deformation theory for the free vibration of cross-ply thick laminated composite cylindrical shells with combinations of clamped, free, and simply supported boundary conditions. The method is used to obtain the dynamic stiffness matrix in order to determine natural frequencies of laminated composite shells which takes into account both the rotary inertia and shear deformations effects. The accuracy of the present model is numerically evaluated by comparing the solutions with those obtained by using the conventional FEM or analytical method.

## 2. FORMULATION OF THICK CROSS-PLY LAMINATED COMPOSITE CYLINDRICAL SHELLS

### 2.1. Kinematics of cylindrical shells

Consider a thick circular cylindrical shell of length  $L$ , thickness  $h$  and radius  $R$  (see Fig.1). The shell consists of a finite number of layers which are perfectly bonded together. Following Reissner-Mindlin assumption, the displacement components are assumed to be

$$\begin{aligned} u(x, \theta, z, t) &= u_0(x, \theta, t) + z\phi_x(x, \theta, t), \\ v(x, \theta, z, t) &= v_0(x, \theta, t) + z\phi_\theta(x, \theta, t), \\ w(x, \theta, z, t) &= w_0(x, \theta, t), \end{aligned} \quad (1)$$

where  $u$ ,  $v$  and  $w$  are the displacement components in the  $x$ ,  $\theta$  and  $z$  directions, respectively,  $u_0$  and  $v_0$  are the in-plane displacements of the shell in the mid-plane, and  $\phi_x$  and  $\phi_\theta$  are the shear rotations of any point on the middle surface of the shell. The strain-displacement

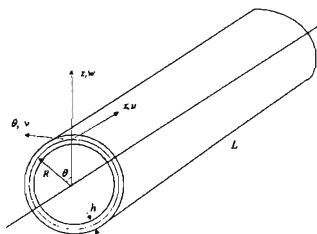


Fig. 1. Laminated composite cylindrical shell

relations of cylindrical shell of radius  $R$  can be written as

$$\begin{aligned} \varepsilon_x &= \frac{\partial u_0}{\partial x} + z \frac{\partial \phi_x}{\partial x}, \quad \varepsilon_\theta = \frac{1}{R} \frac{\partial v_0}{\partial \theta} + \frac{z}{R} \frac{\partial \phi_\theta}{\partial \theta} + \frac{w_0}{R}, \\ \gamma_{x\theta} &= \frac{1}{R} \frac{\partial u_0}{\partial \theta} + \frac{\partial v_0}{\partial x} + z \left( \frac{1}{R} \frac{\partial \phi_x}{\partial \theta} + \frac{\partial \phi_\theta}{\partial x} \right), \\ \gamma_{xz} &= \phi_x + \frac{\partial w_0}{\partial x}, \quad \gamma_{\theta z} = \phi_\theta + \frac{1}{R} \frac{\partial w_0}{\partial \theta} - \frac{v_0}{R}. \end{aligned} \quad (2)$$

## 2.2. Lamina constitutive relations

Consider a composite shell composed of  $N$  orthotropic layers of uniform thickness with the principal material axis of the  $k^{\text{th}}$  layer is oriented at an angle  $\alpha$  with the  $x$  axis. The stress-strain relations of the  $k^{\text{th}}$  layer by neglecting the transverse normal strain and stress, are written as

$$\begin{Bmatrix} \sigma_x^{(k)} \\ \sigma_\theta^{(k)} \\ \tau_{x\theta}^{(k)} \\ \tau_{xz}^{(k)} \\ \tau_{\theta z}^{(k)} \end{Bmatrix} = \begin{bmatrix} \bar{Q}_{11}^{(k)} & \bar{Q}_{12}^{(k)} & \bar{Q}_{16}^{(k)} & 0 & 0 \\ \bar{Q}_{12}^{(k)} & \bar{Q}_{22}^{(k)} & \bar{Q}_{26}^{(k)} & 0 & 0 \\ \bar{Q}_{16}^{(k)} & \bar{Q}_{26}^{(k)} & \bar{Q}_{66}^{(k)} & 0 & 0 \\ 0 & 0 & 0 & \bar{Q}_{44}^{(k)} & \bar{Q}_{45}^{(k)} \\ 0 & 0 & 0 & \bar{Q}_{45}^{(k)} & \bar{Q}_{55}^{(k)} \end{bmatrix} \begin{Bmatrix} \varepsilon_x^{(k)} \\ \varepsilon_\theta^{(k)} \\ \gamma_{x\theta}^{(k)} \\ \gamma_{xz}^{(k)} \\ \gamma_{\theta z}^{(k)} \end{Bmatrix} \quad (3)$$

where  $\bar{Q}_{ij}^{(k)}$  are the transformed stiffness and  $Q_{ij}$  are the lamina stiffness referred to principal material coordinates of the  $k^{\text{th}}$  lamina [22].

## 2.3. Stress and moment resultants

The stress and moment resultants are given by

$$(N_x, N_\theta, N_{x\theta}, Q_x, Q_\theta) = \int_z (\sigma_x, \sigma_\theta, \tau_{x\theta}, \tau_{xz}, \tau_{\theta z}) dz, \quad (4)$$

$$(M_x, M_\theta, M_{x\theta}) = \int_z (\sigma_x, \sigma_\theta, \tau_{x\theta}) z dz \quad (5)$$

The laminate constitutive relations become

$$\begin{Bmatrix} \{N\} \\ \{M\} \end{Bmatrix} = \begin{bmatrix} [A] & [B] \\ [B] & [D] \end{bmatrix} \begin{Bmatrix} \{\epsilon\} \\ \{\gamma\} \end{Bmatrix} \text{ and } \begin{Bmatrix} Q_\theta \\ Q_x \end{Bmatrix} = K \begin{bmatrix} A_{44} & A_{45} \\ A_{45} & A_{55} \end{bmatrix} \begin{Bmatrix} \gamma_{\theta z} \\ \gamma_{xz} \end{Bmatrix} \quad (6)$$

in which the laminate stiffness coefficients ( $A_{ij}$ ,  $B_{ij}$ ,  $D_{ij}$ ) are defined by

$$\begin{aligned} A_{ij} &= \sum_{k=1}^N \bar{Q}_{ij}^k (z_{k+1} - z_k), \quad (i, j = 1, 2, 4, 5, 6) \\ B_{ij} &= \frac{1}{2} \sum_{k=1}^N \bar{Q}_{ij}^k (z_{k+1}^2 - z_k^2), \quad (i, j = 1, 2, 6) \\ D_{ij} &= \frac{1}{3} \sum_{k=1}^N \bar{Q}_{ij}^k (z_{k+1}^3 - z_k^3), \quad (i, j = 1, 2, 6) \end{aligned} \quad (7)$$

with  $K = 5/6$ : the shear correction factor,  $z_{k-1}$  and  $z_k$  are boundaries of the  $k^{\text{th}}$  layer.

For general cross-ply composite laminated cylindrical shells ( $A_{16} = A_{26} = A_{45} = B_{16} = B_{26} = D_{16} = D_{26} = 0$ ), forces and moment resultants are determined by [22]

$$\begin{aligned} N_x &= A_{11} \frac{\partial u_0}{\partial x} + A_{12} \left( \frac{\partial v_0}{R \partial \theta} + \frac{w_0}{R} \right) + B_{11} \frac{\partial \phi_x}{\partial x} + B_{12} \frac{\partial \phi_\theta}{R \partial \theta}, \\ N_\theta &= A_{12} \frac{\partial u_0}{\partial x} + A_{22} \left( \frac{\partial v_0}{R \partial \theta} + \frac{w_0}{R} \right) + B_{12} \frac{\partial \phi_x}{\partial x} + B_{22} \frac{\partial \phi_\theta}{R \partial \theta}, \\ N_{x\theta} &= A_{66} \left( \frac{\partial v_0}{\partial x} + \frac{\partial u_0}{R \partial \theta} \right) + B_{66} \left( \frac{\partial \phi_\theta}{\partial x} + \frac{\partial \phi_x}{R \partial \theta} \right), \\ M_x &= B_{11} \frac{\partial u_0}{\partial x} + B_{12} \left( \frac{\partial v_0}{R \partial \theta} + \frac{w_0}{R} \right) + D_{11} \frac{\partial \phi_x}{\partial x} + D_{12} \frac{\partial \phi_\theta}{R \partial \theta}, \\ M_\theta &= B_{12} \frac{\partial u_0}{\partial x} + B_{22} \left( \frac{\partial v_0}{R \partial \theta} + \frac{w_0}{R} \right) + D_{12} \frac{\partial \phi_x}{\partial x} + D_{22} \frac{\partial \phi_\theta}{R \partial \theta}, \\ M_{x\theta} &= B_{66} \left( \frac{\partial v_0}{\partial x} + \frac{\partial u_0}{R \partial \theta} \right) + D_{66} \left( \frac{\partial \phi_\theta}{\partial x} + \frac{\partial \phi_x}{R \partial \theta} \right), \\ Q_x &= K A_{55} \left( \phi_x + \frac{\partial w_0}{\partial x} \right) \\ Q_\theta &= K A_{44} \left( \phi_\theta + \frac{\partial w_0}{R \partial \theta} - \frac{v_0}{R} \right). \end{aligned} \quad (8)$$

## 2.4. Equation of motions

The equations of motions of the first-order shear deformation shell theory for a thick laminated circular cylindrical shell are [22]

$$\begin{aligned}
 \frac{\partial N_x}{\partial x} + \frac{1}{R} \frac{\partial}{\partial \theta} \left( N_{x\theta} - \frac{1}{2R} M_{x\theta} \right) &= I_0 \frac{\partial^2 u_0}{\partial t^2} + I_1 \frac{\partial^2 \phi_x}{\partial t^2} \\
 \frac{\partial}{\partial x} \left( N_{x\theta} + \frac{1}{2R} M_{x\theta} \right) + \frac{\partial N_\theta}{R \partial \theta} + \frac{Q_\theta}{R} &= I_0 \frac{\partial^2 v_0}{\partial t^2} + I_1 \frac{\partial^2 \phi_\theta}{\partial t^2} \\
 \frac{\partial Q_x}{\partial x} + \frac{\partial Q_\theta}{R \partial \theta} - \frac{N_\theta}{R} &= I_0 \frac{\partial^2 w_0}{\partial t^2} \\
 \frac{\partial M_x}{\partial x} + \frac{\partial M_{x\theta}}{R \partial \theta} - Q_x &= I_1 \frac{\partial^2 u_0}{\partial t^2} + I_2 \frac{\partial^2 \phi_x}{\partial t^2} \\
 \frac{\partial M_{x\theta}}{\partial x} + \frac{\partial M_\theta}{R \partial \theta} - Q_\theta &= I_1 \frac{\partial^2 v_0}{\partial t^2} + I_2 \frac{\partial^2 \phi_\theta}{\partial t^2}
 \end{aligned} \tag{9}$$

where:

$$I_i = \sum_{k=1}^N \int_{z_k}^{z_{k+1}} \rho^{(k)} z^i dz, \quad (i = 0, 1, 2) \tag{10}$$

in which  $\rho^{(k)}$  is the material mass density of the  $k^{\text{th}}$  layer.

## 3. CONTINUOUS ELEMENT METHOD FOR VIBRATION ANALYSIS OF THICK LAMINATED COMPOSITE CYLINDRICAL SHELLS

### 3.1. Strong formulation

For natural vibration of the cylindrical shell, displacements and forces resultants can be expressed by series of Levy [22].

$$\begin{aligned}
 \begin{Bmatrix} u_0(x, \theta, t) \\ v_0(x, \theta, t) \\ w_0(x, \theta, t) \\ \phi_x(x, \theta, t) \\ \phi_\theta(x, \theta, t) \end{Bmatrix} &= \sum_{m=1}^{\infty} \begin{Bmatrix} u_m(x) \cos(m\theta) \\ v_m(x) \sin(m\theta) \\ w_m(x) \cos(m\theta) \\ \phi_{xm}(x) \sin(m\theta) \\ \phi_{\theta m}(x) \cos(m\theta) \end{Bmatrix} e^{i\omega t} \\
 \begin{Bmatrix} N_x(x, \theta, t) \\ N_{x\theta}(x, \theta, t) \\ M_x(x, \theta, t) \\ M_{x\theta}(x, \theta, t) \\ Q_x(x, \theta, t) \end{Bmatrix} &= \sum_{m=1}^{\infty} \begin{Bmatrix} N_{xm}(x) \cos(m\theta) \\ N_{x\theta m}(x) \sin(m\theta) \\ M_{xm}(x) \cos(m\theta) \\ M_{x\theta m}(x) \sin(m\theta) \\ Q_{xm}(x) \cos(m\theta) \end{Bmatrix} e^{i\omega t} \\
 \begin{Bmatrix} N_\theta(x, \theta, t) \\ M_\theta(x, \theta, t) \\ Q_\theta(x, \theta, t) \end{Bmatrix} &= \sum_{m=1}^{\infty} \begin{Bmatrix} N_{\theta m}(x) \cos(m\theta) \\ M_{\theta m}(x) \cos(m\theta) \\ Q_{\theta m}(x) \sin(m\theta) \end{Bmatrix} e^{i\omega t}
 \end{aligned} \tag{11}$$

The vector  $\{y\}_m^T = \{u_m, v_m, w_m, \phi_{xm}, \phi_{\theta m}, N_{xm}, N_{x\theta m}, Q_{xm}, M_{xm}, M_{x\theta m}\}^T$  is called state vector. By replacing expressions (11) into (8) and (9), 13 equations depending only

on variable  $x$  will be obtained. Next,  $N_{\theta m}$ ,  $M_{\theta m}$  and  $Q_{\theta m}$  will be expressed as functions of  $u_m$ ,  $v_m$ ,  $w_m$ ,  $\phi_{zm}$ ,  $\phi_{ym}$ ,  $N_{zm}$ ,  $N_{x\theta m}$ ,  $Q_{zm}$ ,  $M_{zm}$ ,  $M_{x\theta m}$  by using relation (8). Then, the derivations of state vector with respect to variable  $x$  are calculated from equations (8) and (9), after some manipulations

$$\begin{aligned}
 \frac{du_m}{dx} &= f_1(v_m, w_m, \phi_{\theta m}, N_{zm}, M_{zm}) & \frac{dN_{zm}}{dx} &= f_6(u_m, \phi_{zm}, N_{x\theta m}, M_{x\theta m}, \omega) \\
 \frac{dv_m}{dx} &= f_2(u_m, N_{x\theta m}, M_{x\theta m}) & \frac{dN_{x\theta m}}{dx} &= f_7(v_m, w_m, \phi_{\theta m}, N_{zm}, M_{zm}, \omega) \\
 \frac{dw_m}{dx} &= f_3(\phi_{zm}, Q_{zm}) & \frac{dQ_{zm}}{dx} &= f_8(v_m, w_m, \phi_{\theta m}, N_{zm}, M_{zm}, \omega) \\
 \frac{d\phi_{zm}}{dx} &= f_4(v_m, w_m, \phi_{\theta m}, N_{zm}, M_{zm}) & \frac{dM_{zm}}{dx} &= f_9(u_m, \phi_{zm}, Q_{zm}, M_{x\theta m}) \\
 \frac{d\phi_{\theta m}}{dx} &= f_5(\phi_{zm}, N_{x\theta m}, M_{x\theta m}) & \frac{dM_{x\theta m}}{dx} &= f_{10}(v_m, w_m, \phi_{\theta m}, N_{zm}, M_{zm}, \omega)
 \end{aligned} \tag{12}$$

Equations (12) are written in the matrix form for each circumferential mode  $m$

$$\frac{d\{y\}_m^T}{dx} = [A]_m \{y\}_m^T, \quad \text{where } [A]_m \text{ is a } 10 \times 10 \text{ matrix.} \tag{13}$$

### 3.2. Dynamic transfer matrix, dynamic stiffness matrix $[K(\omega)]$

The dynamic transfer matrix  $[T]_m$  is given by

$$[T]_m = e^{[A]_m L} \tag{14}$$

Then  $[T]_m$  is separated into four blocks

$$[T]_m = \begin{bmatrix} T_{11} & T_{12} \\ T_{21} & T_{22} \end{bmatrix} \tag{15}$$

Finally, the dynamic stiffness matrix  $[K(\omega)]_m$  is determined by [19]

$$[K(\omega)]_m = \begin{bmatrix} T_{12}^{-1} T_{11} & -T_{12}^{-1} \\ T_{21} - T_{22} T_{12}^{-1} T_{11} & T_{22} T_{12}^{-1} \end{bmatrix}_m \tag{16}$$

The natural frequencies is calculated from the determinant of the dynamic stiffness matrix  $[K(\omega)]_m$ . For example,

- Free-free boundary condition:  $\det(K) = 0$ .
- Clamped-clamped boundary condition:  $\det(T_{12}) = 0$ .

### 3.3. Assembly of dynamic stiffness matrices

The dynamic stiffness matrix can be easily assembled with other element matrices in order to model a long cylindrical structure, cylinders with portions of different properties or to overcome the problem of numerical instability relating to the too long length of the element.

The assembly procedure of the finite element method is used here. Fig. 2 illustrates an example of assembly for two dynamic stiffness matrices. The global dynamic stiffness

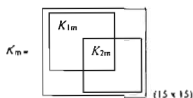


Fig. 2. Assembly of two cylindrical shell continuous elements

matrix  $[K(\omega)]_m$  of a cross ply composite cylindrical shell structure is constructed from two elements  $[K_1(\omega)]_m$  and  $[K_2(\omega)]_m$  assembled along a common edge.

#### 4. NUMERICAL RESULTS AND DISCUSSION

##### 4.1. Validation of present study

A computer program based on Matlab is developed using the CEM to solve a number of numerical examples on free vibration of composite cylindrical shells with different boundary conditions.

Table 1. Comparison of frequency parameters  $\Omega = \omega R(\rho/E_2)^{1/2}$  of cross-ply shells simply supported at both ends (three-layers,  $h/R = 0.02$ ,  $L/R = 4$ , Material 1)

Lamination (outer/inner)	References	$\Omega_1$	$\Omega_2$	$\Omega_3$ ( $\times 10^{-2}$ )	$\Omega_4$	$\Omega_5$
0°/0°/0°	Narita [9]	14.39	16.32	17.42	21.46	26.65
	CEM	14.37	16.30	17.41	21.41	26.64
	Differences (%)	0, 14	0, 12	0, 06	0, 23	0, 04
0°/90°/0°	Narita [9]	14.82	16.46	18.73	25.73	25.79
	CEM	14.82	16.46	18.73	25.69	25.77
	Differences (%)	0, 00	0, 00	0, 00	0, 16	0, 08
90°/90°/0°	Narita [9]	16.10	21.21	22.62	31.20	32.44
	CEM	15.99	21.08	22.59	30.93	32.28
	Differences (%)	0, 69	0, 62	0, 13	0, 87	0, 50
0°/0°/90°	Narita [9]	17.16	17.47	23.90	25.82	31.49
	CEM	17.11	17.41	23.81	25.78	31.36
	Differences (%)	0, 29	0, 34	0, 38	0, 16	0, 41
90°/0°/90°	Narita [9]	21.35	23.54	33.60	40.18	41.40
	CEM	21.25	23.52	33.31	40.02	41.07
	Differences (%)	0, 47	0, 09	0, 87	0, 40	0, 80

In this example, the natural frequencies are calculated for cross-ply laminated cylindrical shells having small thickness ratio ( $h/R = 0.02$ ) and moderate length ( $L/R = 4$ ).

The shell has three-layer cross-ply from outer layer to inner. All layers are of equal thickness and material properties used are:  $E_1 = 138$  GPa,  $E_2 = 8.96$  GPa,  $G_{12} = G_{13} = 7.1$  GPa,  $G_{23} = 3.45$  GPa,  $\nu_{12} = 0.3$ ,  $\rho = 1645$  kg/m<sup>3</sup>, Material 1.

In numerical examples, the frequency parameters are defined as  $\Omega = \omega R(\rho/E_2)^{1/2}$  and are presented for two edge conditions: simply supported and clamped-free. The present values are compared with the corresponding FE solutions given by Narita [9] in Tab. 1-2.

Table 2 Comparison of frequency parameters  $\Omega = \omega R(\rho/E_2)^{1/2}$  of cantilevered (clamped-free) cross-ply shells (three-layers,  $h/R = 0.02$ ,  $L/R = 4$ , Material 1)

Lamination (outer/inner)	References	$\Omega_1$	$\Omega_2$	$\Omega_3$ ( $\times 10^{-2}$ )	$\Omega_4$	$\Omega_5$
0°/90°/0°	Narita [9]	8.442	11.30	11.51	17.25	20.79
	CEM	<b>8.439</b>	<b>11.29</b>	<b>11.51</b>	<b>19.23</b>	<b>20.75</b>
	Differences (%)	0,04	0,09	0,00	5,68	0,19
0°/0°/0°	Narita [9]	8.453	9.732	12.33	14.17	20.31
	CEM	<b>8.449</b>	<b>9.724</b>	<b>12.33</b>	<b>14.15</b>	<b>20.27</b>
	Differences (%)	0,05	0,08	0,00	0,14	0,20
0°/0°/90°	Narita [9]	9.535	11.56	14.38	22.28	22.34
	CEM	<b>9.641</b>	<b>11.62</b>	<b>14.23</b>	<b>22.11</b>	<b>22.20</b>
	Differences (%)	1,11	0,52	1,04	0,76	0,63
90°/90°/0°	Narita [9]	10.09	11.49	20.05	20.53	23.61
	CEM	<b>10.31</b>	<b>11.63</b>	<b>20.24</b>	<b>20.77</b>	<b>25.00</b>
	Differences (%)	2,18	1,22	0,95	1,17	5,89
90°/0°/90°	Narita [9]	11.25	17.70	20.66	27.69	32.67
	CEM	<b>11.24</b>	<b>17.62</b>	<b>20.66</b>	<b>27.59</b>	<b>32.39</b>
	Differences (%)	0,09	0,45	0,00	0,36	0,86

It can be shown from Tab. 1-2 that the frequencies obtained by CEM of composite cylindrical shells subjected to different boundary conditions are in an extremely good agreement with those of Narita calculated by FEM.

The present values are compared with the results obtained by 3-D analysis, parabolic shear deformation, constant shear deformation and thin shell theory [6]. The comparison of the fundamental frequency  $\omega^* = gh(\rho\pi^2G_{12})^{1/2}$  for various thickness-radius ratios ( $h/R$ ) with those results using 3-D analysis obtained by Ye and Soldatos [1], for simply supported cylindrical shells with symmetric cross-ply laminates is presented in Tab. 3. The properties for the comparison are  $R/L = g$ ,  $E_1/E_2 = 40$ ,  $G_{12} = 0.6E_2$ ,  $G_{13} = G_{23} = 0.5E_2$ ,  $\nu_{12} = 0.25$ , Material 2.

The agreement correlated with the previously published results is given in the Tabs. 1-3. which indicates that the present analysis is accurate.

Table 3. Comparison of the fundamental frequency  $\omega^* = gh(\rho\pi^2G_{12})^{1/2}$  of simply supported cylindrical shells with symmetric cross-ply laminates by different methods ( $R/L = 1$ , Material 2).

$h/R$	$0^\circ/90^\circ/90^\circ/0^\circ$			$90^\circ/0^\circ/0^\circ/90^\circ$		
	Viswanathan[6]	Ye [3]	CEM	Viswanathan[6]	Ye [3]	CEM
0.1	0.074118	0.064600	<b>0.06397</b>	0.051555	0.052748	<b>0.05310</b>
	0.076309	0.066335	<b>0.06566</b>	0.054261	0.059130	<b>0.05907</b>
	0.082831	0.079277	<b>0.07888</b>	0.062899	0.070738	<b>0.07089</b>
0.2	0.170696	0.162844	<b>0.15890</b>	0.121318	0.130168	<b>0.13325</b>
	0.176990	0.170868	<b>0.16825</b>	0.152241	0.150651	<b>0.15267</b>
	0.177462	0.175188	<b>0.17256</b>	0.163189	0.158886	<b>0.15915</b>
0.3	0.275497	0.263048	<b>0.25464</b>	0.231831	0.218779	<b>0.22732</b>
	0.280720	0.272860	<b>0.26688</b>	0.244864	0.236385	<b>0.24281</b>
	0.294626	0.283798	<b>0.27974</b>	0.284595	0.268258	<b>0.26990</b>

#### 4.2. Harmonic responses of Clamped-free composite cylindrical shell

In Fig. 3, the harmonic response obtained with 3 continuous elements is compared with those obtained with 144 ( $24 \times 6$  mesh) and 900 finite elements ( $60 \times 15$  mesh) of ANSYS SHELL 99 for clamped-free ( $0^\circ/90^\circ/90^\circ/0^\circ$ ) cylindrical shell, ( $h = 0.0254$  m,  $R/h = 20$ ,  $L/R = 2$ , Material 1)

With  $24 \times 6$  mesh, there is a convergence of results obtained with CEM and FEM up to 567.6 Hz. Beyond this limit, there is a discrepancy which can be explained by the fact that the meshing in FE idealization is not fine enough. An excellent convergence is noted for CEM and FEM with 900 elements ( $60 \times 15$  mesh).

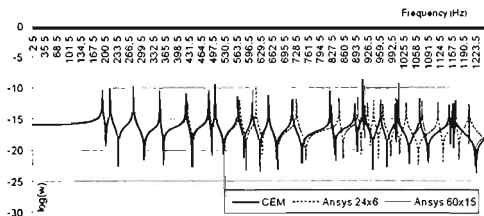


Fig. 3. Comparison of harmonic responses of clamped-free composite cylindrical shell ( $0^\circ/90^\circ/90^\circ/0^\circ$ ) by CEM and by FEM with different mesh ( $h = 0.0254$  m,  $R/h = 20$ ,  $L/R = 2$ , Material 1)

A good similarity can be observed between the three curves of harmonic responses of free-free ( $0^\circ/90^\circ/0^\circ/90^\circ$ ) composite cylindrical shell by CEM and by FEM with  $24 \times 6$  and  $60 \times 15$  meshes in Fig. 4, Material 3:  $E_1 = 138.6$  GPa,  $E_2 = 8.27$  GPa,  $G_{12} = 4.12$  GPa,  $G_{13} = G_{23} = 0.6E_2$ ,  $\nu_{12} = 0.26$ ,  $\rho = 1824$  kg/m<sup>3</sup>.

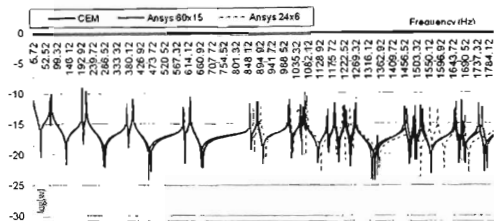


Fig. 4. Comparison of harmonic responses of free-free ( $0^\circ/90^\circ/0^\circ/90^\circ$ ) by CEM and by FEM with different mesh ( $h = 0.0254$  m,  $R/h = 20$ ,  $L/R = 1$ , Material 3)

Some first natural frequencies for clamped-free ( $0^\circ/90^\circ/90^\circ/0^\circ$ ) composite cylindrical shell calculated by CEM and FEM are compared in Tab. 4.

Table 4. Natural frequencies for clamped-free composite cylindrical shell ( $0^\circ/90^\circ/90^\circ/0^\circ$ ),  $h = 0.0254$  m,  $R/h = 20$ ,  $L/R = 2$

Mode	$m$	CEM (Hz)	Ansys $24 \times 6$ (Hz)	Errors (%)	Ansys $60 \times 15$ (Hz)	Errors (%)
1	3	<b>194.26</b>	194.43	0,09	194.24	0,01
2	2	<b>215.45</b>	215.45	0,00	215.46	0,00
3	4	<b>278.68</b>	279.7	0,37	278.97	0,10
4	1	<b>351.45</b>	351.44	0,00	351.48	0,01
5	5	<b>423.57</b>	427.26	0,87	424.57	0,24
6	4	<b>486.07</b>	488.17	0,43	486.47	0,08
7	3	<b>503.49</b>	504.41	0,18	503.68	0,04
8	5	<b>567.6</b>	572.67	0,89	568.72	0,20
9	6	<b>607.27</b>	617.48	1,68	609.53	0,37
10	2	<b>652.55</b>	653.07	0,08	652.83	0,04
11	6	<b>717.87</b>	729.88	1,67	720 4	0,35
12	7	<b>823.47</b>	847.42	2,91	827 79	0,52
13	4	<b>890.74</b>	899.43	0,98	892.86	0,24
14	5	<b>912.5</b>	926.2	1,50	915.42	0,32
15	7	<b>916.01</b>	942.38	2,88	920.79	0,52

Next, the comparisons of computing time by FEM and by CEM using the same computer are shown in Tab. 5 and Tab. 6.

Table 5. Computing time for free-free composite cylindrical shells ( $0^\circ/90^\circ/0^\circ/90^\circ$ )

FEM ( $24 \times 6$ )	FEM ( $60 \times 15$ )	CEM ( $m = 3$ )
600 s	5880 s	30 s

Table 6. Computing time for clamped-free composite cylindrical shells ( $0^\circ/90^\circ/90^\circ/0^\circ$ )

FEM ( $24 \times 6$ )	FEM ( $60 \times 15$ )	CEM ( $m = 3$ )
720 s	5280 s	72 s

Advantages of CEM are confirmed in Tab. 5 and Tab. 6. Using only 3 continuous elements for meshing, CEM accelerates the calculation speed and save data storage capacity of computers. For the FEM model, it takes much more time to solve the problem if we refine the meshing in order to have more exact result.

#### 4.3. Influences of some parameters on frequency of composite cylindrical shell

The effects of thickness-to radius ratios, length-to radius ratios and the number of layers on the frequencies of composite cylindrical shell are presented in Figs 5-6, Fig. 7 and Fig. 8, respectively.

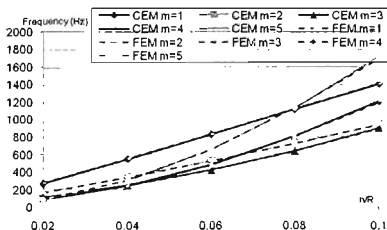


Fig. 5. Effect of  $h/R$  on simply supported composite cylindrical shell ( $0^\circ/90^\circ/90^\circ/0^\circ$ ,  $h = 0.0254$  m,  $L/R = 2$ , Material 1) by CEM and by FEM

From Fig. 5 and Fig. 6, it is seen that the raise of the shell thickness will result in the increasing of natural frequencies of the shell. The frequency decreases in general as  $L/R$  increases. The decrease is fast for very short shells (Fig. 7). With the same shell thickness, when the number of layers increases, natural frequency increases (Fig. 8). This confirms influence of the arrangement of material layers to the vibration of composite shell.

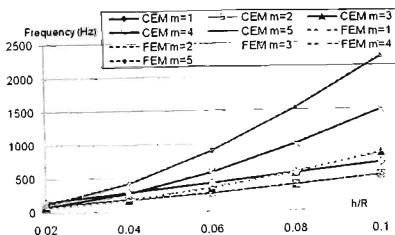


Fig. 6 Influences of  $h/R$  on clamped-free composite cylindrical shell ( $0^\circ/90^\circ/0^\circ/90^\circ$ ,  $h=0.0254$ ,  $L/R=2$ , Material 1) by CEM and by FEM

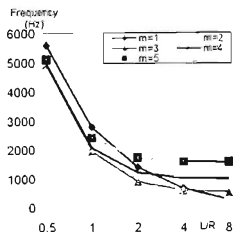


Fig. 7 Effect of  $L/R$  on simply supported composite cylinder ( $0^\circ/90^\circ/90^\circ/0^\circ$ ,  $h = 0.0254$  m,  $L/R = 0.1$ , Material 1)

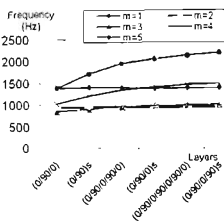


Fig. 8 Influence of number of layers on simply supported composite cylinder ( $h = 0.0254$  m,  $h/R = 0.1$ ,  $L = 2R$ , Material 1)

## 5. CONCLUSIONS

This article has succeeded in constructing the CEM model and in creating a computing program by Matlab to solve the problem of vibration of thick composite cylindrical shells using Continuous Element Method. Through different comparisons with the published results and with the other calculation methods, the obtained results are very satisfied.

Numerical results of this research show that CEM allows to compute the natural frequencies of thick laminated cylindrical shells with high accuracy, within the studied frequency range. Using minimum meshing, this method increases the calculation speed and economics the storage capacity of computers. In this paper, only in-axis composite

shells are studied. But actually, there is no limitation on the manner of ply angles of the lamina. Those problems can also be solved by using CEM.

### ACKNOWLEDGEMENTS

This work was supported by the NAFOSTED of Vietnam, Project 107.02-2011.08.

### REFERENCES

- [1] Dukumaci E., An exact solution for coupled bending and torsion vibrations of uniform beams having single cross-section symmetry, *Journal Sound Vibration*, **119**(3), (1987), 443-9.
- [2] Liu B., Xing Y. F., Qatu M. S., Ferreira AJM, Exact characteristic equations for free vibrations of thin orthotropic circular cylindrical shells. *Composite structures*, **94**, (2012), 484-493.
- [3] Ye J. and Soldatos K. P., Three-dimensional vibration of laminated cylinders and cylindrical panels with symmetric or antisymmetric cross-ply lay-up, *Comp. Engg*, **4**, (1994), 429-444.
- [4] Khdeir A. A., Reddy J. N. and Fredrick D., A study of bending, vibration and buckling of cross-ply circular cylindrical shells with various shells theories, *International Journal of Engineering Science*, **11**(27), (1989), 1337-1351.
- [5] Li J., Shen R., Hua H., Jin X., Bending-torsional coupled dynamic response of axially loaded composite Timoshenko thin-walled beam with closed cross section, *Composite Structures*, **64**, (2004), 23-35.
- [6] Viswanathan K. K., Kim K. S., Lee J. H., Koh H. S. and Lee J. B., Free vibration of multi-layered circular cylindrical shell with cross-ply walls, including shear deformation by using spline function method *Journal of Mechanical Science and Technology*, **22**, (2008), 2062-2075.
- [7] Mei C., Effect of material coupling on wave vibration of composite Timoshenko beams, *Journal of Vibration Acoustics*, **127**, (2005), 333-40.
- [8] Sinha S. K., Combined torsional-bending-axial dynamics of twisted rotating cantilever Timoshenko beam with contact-impact loads at the free end, *Journal of Applied Mechanics*, **74**, (2007), 505-22.
- [9] Nariya Y., Ohta Y., Saito M., Finite element study for natural frequencies of cross-ply laminated cylindrical shells, *Composite structures*, **26**, (1993), 55-62.
- [10] Ganapathi M., Patel B. P., Pawargi DS, Dynamic analysis of laminated cross-ply composite non-circular thick cylindrical shells using higher-order theory, *International Journal of Solids and Structures*, **39**, (2002): 5945-5962.
- [11] Von Flotow A. H., The acoustic limit of control of structural dynamics. In: Atluri S, Amos T, editors. *Large space structures: dynamics and control*, Berlin: Springer, (1987), 213-37
- [12] Nayfeh A. M., Hefzy M. S., Continuum modeling of the mechanical and thermal behavior of discrete large structures, *AIAA J*, **19**(6), (1978), 766-73.
- [13] Lee U., Equivalent continuum models of large plate like lattice structures, *International Journal Solids and Structure*, **31**(4), (1994), 457-67.
- [14] Banerjee J. R., Williams F. W., Coupled bending-torsional dynamic stiffness matrix of an axially loaded Timoshenko beam element, *International Journal of Solids and Structures*, **31**(6), (1994), 749-62.
- [15] Pestel E. C., Leckie F. A., Matrix methods in elasto-mechanics, New York: McGraw-Hill, (1993).
- [16] Yong Y., Lin Y. K., Dynamics of complex truss-type space structures, *AIAA J*, **28**(7), (1989), 1250-8.

- [17] Lee U., Spectral element method in structural dynamics. Singapore: John Wiley & Sons, (2009).
- [18] Casimir J. B., Kevorkian S., Vinh T., The dynamic stiffness matrix of two-dimensional elements: application to Kirchhoff's plate continuous element, *Journal Sound Vibration*, **287**, (2005), 571–89.
- [19] Casimir J. B., Nguyen M. C., Tawfiq I., Thick shells of revolution: derivation of the dynamic stiffness matrix of continuous elements and application to a tested cylinder, *Comput Struct*, **85**, (2007), 1845–57.
- [20] Khadimallah M. A., Casimir J. B., Chafra M., Smaoui H., Dynamic stiffness matrix of an axisymmetric shell and response to harmonic distributed loads, *Comput Struct*, **89**, (2011), 467–475.
- [21] Casimir J. B., Duforet C., Vinh T., Dynamic behaviour of structures in large frequency range by continuous element methods. *Journal Sound Vibration*, **267**, (2003), 1085–106.
- [22] Reddy J. N., Mechanics of laminated composite plates and shells, *Theory and Analysis*, (2004), CRC Press.

*Received July 31, 2012*